

Supramolecular Catalysis | Very Important Paper |

VIP

Hydrolytic Nanozymes

Luca Gabrielli,^[a] Leonard J. Prins,^[a] Federico Rastrelli,^[a] Fabrizio Mancin,^[a] and Paolo Scrimin^{*,[a]}

In memory of Umberto Tonellato, the scientific father of our group

Abstract: In 2004 we first reported catalytic nanoparticles, that are able to cleave phosphate diesters with very high efficiency (*Angew. Chem. Int Ed*, **2004**, 43, 6165–6169) and dubbed them “nanozymes” for the similarity of their behavior with natural enzymes, both in terms of efficiency and mechanism of action. Since then the field has impressively expanded and a search on the web of science at the time of submitting this contribution returned almost 1,000 entries. This minireview highlights what has been done in the field focusing specifically on hydrolytic nanozymes, the focal point of the research in our group since

its very beginning. Special emphasis is given to the advantage of bringing catalytic units in the confined space of a nanosystem in terms of inducing the cooperation between them, favoring the interaction with substrates, and altering the local environment. We will try to answer to questions like: why can a lipophilic substrate be transformed by these catalysts even in an aqueous environment? Why may the pH in the catalytic loci of the nanosystem be different from that of the bulk solution even in the presence of buffers? Why are most of these nanosystems better than monovalent ones?

1. Introduction

Nanozymes are nanoscale systems endowed with the property of catalyzing a chemical reaction by interacting with the substrate they transform via a pre-transformation complexation process.^[1–5] The reactions follow, hence, the same steps of an enzyme-catalyzed transformation: the equilibrium towards the enzyme/substrate complex (ES) followed by its evolution into products with the final release of the enzyme. The analogy with enzymes is also supported by the dimensions of these systems (typically 2–50 nm), not much different from those of a catalytic protein. As an example, the diameter of trypsin is ca. 5 nm. Most of these nanosystems, are intrinsically multivalent, since they feature a collection of identical (or similar) functionalities.^[6,7] These functional groups may be held together by weak interactions or by covalent bonds. Examples of the first are micellar or vesicular aggregates while examples of the second are functional polymers, dendrimers or monolayer-protected nanoparticles. Multivalency is particularly important in binding. Numerous reports show these systems interact very strongly with

multivalent counterparts. Multivalency is a property well-exploited by natural systems to achieve astonishingly high binding constants just by summing up contributions of several units, individually capable only of a very weak binding interaction. Benefits of these interactions, driven by multivalency, are enhanced selectivity and even specificity in recognition. It is thus not surprising that multivalent systems are able to govern cell-cell, protein–protein, protein–cell interactions, critical processes for the occurrence of life as we know it.^[8] The connection of multivalency to catalysis is obvious, because catalysis requires the binding of the transition state of a reaction thus lowering its energy.^[9] Thus multivalent nanozymes, if properly designed, may enjoy the advantage of a strong interaction with the transition state of the catalyzed reaction. Furthermore, in the catalytic process several functional units may operate in a concerted, cooperative^[10] fashion, often with complementary roles. This last aspect mimics what happens in the catalytic site of natural enzymes. Although natural enzymes are typically not multivalent species, intriguing examples of multivalent enzymes are emerging.^[11]

The minireview discusses two classes of hydrolytic reactions: the hydrolysis of carboxylic- and phosphoric-acid esters. Accordingly, in the different paragraphs several nanosystems performing the same or similar tasks are reported. We have taken advantage of this to highlight, whenever possible, common aspects and differences pertaining to each class of nanosystems discussed.

2. Assessing the Catalytic Performance of Nanozymes

Quite often the assessment of the catalytic performance of a nanozyme is poorly performed and does not allow a correct

[a] Dr. L. Gabrielli, Dr. Prof. L. J. Prins, Dr. Prof. F. Rastrelli, Dr. Prof. F. Mancin, Dr. Prof. P. Scrimin
Department of Chemical Sciences, University of Padova, via Marzolo, 1,
35131 Padova, Italy
E-mail: paolo.scrimin@unipd.it
luca.gabrielli@unipd.it
leonard.prins@unipd.it
federico.rastrelli@unipd.it
fabrizio.mancin@unipd.it
<http://wwwdisc.chimica.unipd.it/paolo.scrimin/pubblica/>
<http://wwwdisc.chimica.unipd.it/leonard.prins/pubblica/>
<http://wwwdisc.chimica.unipd.it/federico.rastrelli/pubblica/>
<http://wwwdisc.chimica.unipd.it/fabrizio.mancin/pubblica/index.htm>
ORCID(s) from the author(s) for this article is/are available on the WWW
under <https://doi.org/10.1002/ejoc.202000356>.

comparison between them and with the reference reaction they are supposed to catalyze. Two issues must be considered when determining the catalytic efficiency of such nanosystems: first, they are multivalent and hence each of them presents several catalytic sites; second, the transformation of a substrate is preceded by its binding to the nanocatalyst, as mentioned in the introduction. Because of their multivalency the concentration of the catalyst must be, whenever this is possible, that of the single catalytic units and not that of the nanosystems. For instance, a 2-nm gold nanoparticle passivated with thiols functionalized each with a metal complex contains ca. 60 of those metal complexes: the concentration of the metal complexes must be considered and not that of the gold nanoparticles unless specific mechanistic considerations dictate other ways. This would be the case of experimental evidence of a dinuclear catalytic site: in that case the above metal complex concentration must be divided by two. Afterwards, the catalytic performance should be determined using the classical Michaelis–Menten

equation. Relevant parameters thus obtained are k_{cat} , the first-order rate constant that evaluates the rate of transformation of the substrate when fully bound to the nanocatalyst and K_M , the reciprocal of the affinity constant of the substrate for the catalyst (assuming a binding equilibrium faster than the rate of product formation). The ratio k_{cat}/K_M has the dimensions of a second order rate constant and is a measure of how efficiently the catalyst converts the substrate into products under subsaturation conditions (it is called “catalytic efficiency” in enzyme catalysis) taking in consideration also the efficiency of its binding. Usually, Michaelis–Menten kinetic analysis is done under conditions of excess substrate over catalyst determining the initial rate constant, v_i . Experimental plots report v_i vs. substrate concentration at a given catalyst concentration ([catalyst] \ll [substrate]). However, not all nanosystems allow to work under those conditions. A notable example is that constituted by micellar (and vesicular) aggregates where operating under those conditions is not feasible for two reasons. First,



Luca Gabrielli received his PhD from the University of Milano-Bicocca (2013), under the supervision of Prof L. Cipolla. After post-doctoral experiences at the group of Prof. F. Mancin (University of Padova, 2014) and at the group of Prof. C. A. Hunter (University of Cambridge, 2017), where he was awarded with an IF-MCS fellowship, he then moved back to the University of Padova (2019), as a temporary assistant professor.



Leonard Prins (1974) is professor in organic chemistry at the University of Padova. He obtained his PhD in 2001 from the University of Twente and carried out postdoctoral research at Caltech and the University of Padova. In 2009 he received the Ciamician medal from the Organic Division of the Italian Chemical Society. His current research interests are non-equilibrium self-assembly, multivalent catalysis and sensing.



Federico Rastrelli received his PhD (2005) from the University of Padova, where he is associate professor. As a post-doc in the group of Prof A. Bagno he has been working on experimental NMR and quantum chemical calculations of NMR parameters in small diamagnetic and paramagnetic molecules as well as on applications of NMR spectroscopy in food chemistry. His present research topics include the design of NMR methods for the investigation of nanosystems and the study of transport phenomena in complex matrices



Fabrizio Mancin received his Ph.D. from the University of Padova in 2000, working under the supervision of prof. U. Tonellato. He is full Professor at the University of Padova since 2016. He was awarded a SCI Organic Division Research Prize in 2014 and an ERC Starting Grant in 2010. His scientific interests are focused on self-organized nanoreceptors, with focus on their applications to sensing and catalysis.



Paolo Scrimin graduated from the University of Padova (1976) where he is full Professor of Organic Chemistry since 1997. He has been the recipient of the Ciamician (1988) and Mangini (2018) medals (awarded by SCI, Organic Division). His scientific interests are focused on nanosystems, particularly on the possibility to exploit cooperativity and trigger new functions within them. He is a member of the Editorial Board of EurJOC

these systems form only above a critical concentration (critical aggregate concentration, cac) and this might require a high concentration for their study. Second and most important, an excess of substrate may change their morphology or even the nature itself of the nanosystem. In these cases, it is mandatory to operate in excess of catalyst with respect to the substrate and experimental plots report k_{obs} vs. catalyst concentration at a given substrate concentration. The constant k_{obs} represents the apparent first order rate constant of the transformation of the substrate into products. When the substrate is fully bound to the catalyst, $k_{obs}=k_{cat}$. However, since we are dealing with multivalent systems, the k_{cat} determined under conditions [catalyst] \ll [substrate], $k_{cat,full}$ or the opposite ([catalyst] \gg [substrate]), $k_{cat,single}$, might be different.^[12] The same is also true for the K_M parameter, of course. In the first case the multivalent catalyst is fully saturated with substrates while in the second case each nanosystem interacts with no more than a single substrate. Even considering as the catalyst concentration that of the single catalytic units present in the multivalent nanocatalyst, under conditions of excess substrate or catalyst, each catalytic site is surrounded by substrate-bound or empty neighbors, respectively. The occupation state of the next neighbor might indeed affect the performance of each individual catalytic site, both from the point of view of its transformation and its binding.

Finally, what parameters should be utilized to compare the performance of the different nanocatalysts? There is not a single answer and different parameters provide different information. When k_{cat} is compared with k_{uncat} (the first order rate constant of the uncatalyzed process) the intrinsic performance of the catalytic process is evaluated in comparison with the reaction in the absence of any catalyst. This is a feasible comparison between two first order rate constants. In the case of hydrolysis this is the reaction in water at a given pH. For an acid or base catalyzed process, it obviously neglects the actual concentration of H^+ or OH^- often overemphasizing the absolute performance of a catalyst. A better comparison would involve taking into considerations these concentrations but that requires the comparison between two second order rate constants. For this reason, the k_{cat}/K_M ratio for the nanozyme is a better parameter. It allows not only the comparison with the “uncatalyzed” process but also with the unimolecular catalyst that constitutes the key functional group in the catalytic site of the nanozyme. For instance, the k_{cat}/K_M of a nanozyme featuring imidazole groups for the catalysis of carboxylate esters hydrolysis can be compared with the second order reaction constant, k_2 , obtained in the presence of imidazole (or substituted imidazole). The k_{cat}/K_M of a nanozyme featuring metal complexes can be compared with the k_2 of the same complex alone.

3. Nanocatalysts for the Hydrolysis of Carboxylic Acid Esters

3.1. Nanoesterases

Nanosystems capable of accelerating the hydrolysis of carboxylate esters are often considered models of esterases. These en-

zymes represent a quite broad family of proteins in which one of the most common traits is the presence of three amino acids in the catalytic site (catalytic triad) playing different and complementary roles:^[13] acid (typically aspartic acid), base (typically histidine) and nucleophile (typically serine). They represent an interesting example of convergent evolution into a highly cooperative class of catalysts. Enzymes operating with only two of these functions are known. The mimicry of these systems has attracted scientists since the very early days of biomimetic chemistry.^[14,15] One of the most studied nanosystems is constituted by micellar aggregates of functionalized surfactants. The topic has been extensively reviewed^[16] and the mechanism of action is fairly well understood.^[17] The most accepted way of analyzing the reactivity within these systems is based on the pseudophase model.^[17,18] In pseudophase treatments, the micellar solution is divided into distinct reaction environments and one attempts to factor-out the transfer equilibria of reactants between solvent and aggregates. The take-home message is that, although impressive, enzyme-like, rate accelerations can be attained with these aggregates, they hardly affect the mechanism of the reference reaction in water. Consequently, most of the effect can be explained by the concentration of reactants in the micellar pseudophase and the change of the polarity of the environment. Among the reactants there may be OH^- ions (as counterions of cationic groups) with consequent change of the local pH. Because of the rapid exchange of the functionalized surfactant between aggregate and bulk water it is difficult to observe cooperativity in these systems. There are notable exceptions, though, and we will discuss a couple of these examples, one relatively old and another one very recent. They will show how the aggregation of an amphiphilic molecule can not only accelerate a reaction but, in addition, change drastically or its mechanism or the occurrence of the reaction itself, something we will discuss subsequently with other nanosystems.

The lipophilic chiral ligand of Figure 1 (left) becomes amphiphilic upon complexation with $Cu(II)$ ions forming micellar aggregates.^[19] These aggregates accelerate the cleavage of esters of α -amino acids with significant enantioselectivity. When the hydrocarbon chain is replaced by a methyl, on the contrary, the complex slows down the cleavage process with insignificant enantioselectivity. The rate acceleration observed in the micelles requires the formation of the ternary complex substrate- $Cu(II)$ -ligand in which the ligand hydroxyl acts as the nucleophile (equilibrium shifted to the left, Figure 1). The partial dehydration of the coordination sphere of the metal ion in the aggregate allows the coordination of this hydroxyl which is replaced by water in the hydrophilic complex (equilibrium shifted to the right, Figure 1). The critical cooperative contribution as a nucleophile of the alcoholic function is lost in the non-aggregated system. As a consequence, the aquo complex is much less reactive and, with the chiral arm not coordinated to the metal, it loses also the enantioselection ability. Thus, the aggregation controls the outcome of the reaction by changing the coordination sphere of the metal ions. Desolvation of functional groups in the catalytic sites of enzymes is considered one of the driving forces for enhancing their catalytic activity.^[20] Compartmentalization and selective solvation are hence peculiar

properties of these nanozymes. On this regards a recent spectacular example of catalysis of a carboxylate ester hydrolysis in a vesicular system was described by Hunter and Williams.^[21] The important aspect of what they reported is not the rate acceleration observed but the possibility to control the movement of a catalyst in different regions of the bilayer of a vesicle and trigger specific endovesicular catalysis. In the inactive system a protein captures the catalyst through an interaction on the outer surface of a vesicle. A competing ligand displaces the protein liberating the catalyst that can reach the interior of the vesicle inducing the catalytic process. The segregation of catalyst, substrate and inhibitor in the vesicular nanoreactor allows the monitoring of events that occur in different regions of the nanosystem.

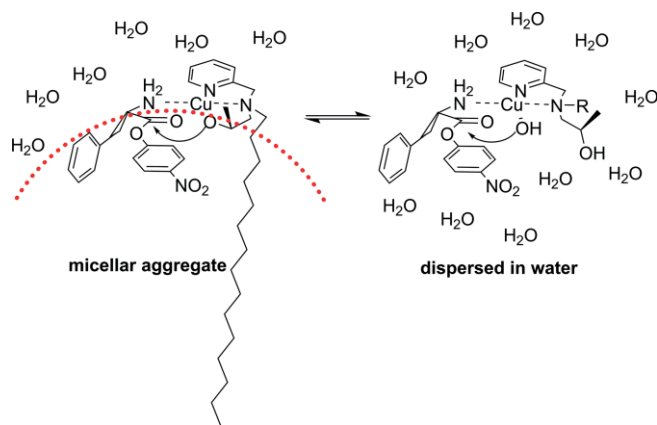


Figure 1. The pyridine-based ligand may adopt two different coordination modes to Cu(II): one with the hydroxyl-bearing arm coordinated to the metal (left) and the other in which that coordination position is replaced by water (right). The position of the equilibrium is controlled by the aggregation state of the complex. The dotted red curve represents the interfacial region between the aggregate and bulk water (adapted from ref.^[19]).

Dendrimers have been dubbed unimolecular micelles^[22,23] as they share several properties with conventional micellar aggregates (multivalency, creation of an environment different from that of the bulk, ability to bind substrates) without the limitations connected to the aggregation process and the requirement of a solvent with specific properties. One of the most interesting examples of dendrimers as catalysts for the cleavage of esters was reported by Raymond's group,^[24,25] who has studied peptide-based systems. The fact that amino acids are used to construct the nanosystem strongly enhances the analogy with enzymes.

Two classes of dendrimers were studied: those endowed with a catalytic site at the core of the nanosystems and those in which the branches were catalytically competent. To identify the best catalysts of the first class they exploited a combinatorial approach to prepare a library of over 65,000 peptide dendrimers. The library was screened on-bead against an anionic fluorogenic ester to pinpoint active sequences. Interestingly they all contained at least one histidine and arginine in the catalytic core and predominantly aromatic residues at the outer positions. The cooperativity emerged in this case from the binding contribution, deriving from the charged cationic groups and the enhanced hydrophobicity of the catalytic site, and the pres-

ence of histidine as a nucleophile/general acid. In the case of catalysis deriving from the peptidic branches (peripheral catalytic groups) a series of peptide-dendrimers of different generation (up to the fourth, Figure 2 and Table 1) containing His-residues in every generation were studied.^[24] An additional Ser-residue was also present as a nucleophilic functional group.

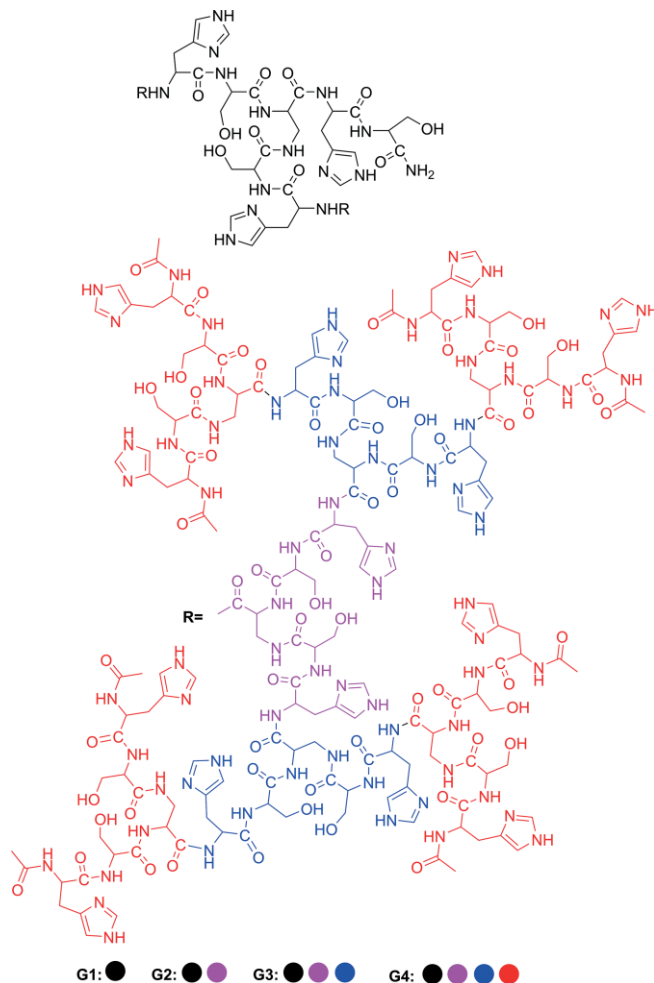


Figure 2. Dendrimers of different generation (G1–4) were prepared as estero-lytic nanozymes by Raymond's group using amino acids as building blocks. The core (in black, top) is surrounded by the arms, R, growing in generation from black and violet (G2), black, violet and blue (G3) and black, violet, blue and red (G4) (adapted from ref.^[24a]).

Table 1. Kinetic parameters^[a] for the cleavage of pyrene trisulfonate butanoyl ester by peptide dendrimers of Figure 2.^[24a]

Dendrimer generation	K_M , μM	k_{cat} , min^{-1}	$k_{\text{cat}}/k_{\text{uncat}}$ ^[b]	k_{cat}/K_M , $\text{M}^{-1}\times\text{min}^{-1}$
G1	450	0.031	2200	69
G2	140	0.11	8000	786
G3	63	0.24	17000	3810
G4	29	0.55	39000	18970

[a] Conditions: 5 mM aq. citrate, pH 5.5, 27 °C. [b] $k_{\text{uncat}} = 1.4 \times 10^{-5}$, min^{-1} .

All dendrimers catalyzed the hydrolysis of active esters following Michaelis–Menten profiles. Comparison of the k_{cat} , K_M , and k_{cat}/K_M values for each generation gave a valuable insight in the cooperativity between functional groups in the den-

dimer deriving from the presence of the imidazoles of the His residues. Comparison with 4-methyl-imidazole showed that with this compound, as the pH increased, the rate acceleration was linked to the deprotonation of the imidazole (the actual nucleophile). On the contrary, for the dendrimer-catalyzed reactions the rate was bell-shaped in the pH range studied (4.5–7.5) indicating the imidazole was acting both as a general acid and as a nucleophile, a typical cooperative process.^[26] The concept of engineered peptide catalysts was recently extended to the functionalization of Merrifield resins with significant evidence of cooperativity between the functional groups of the canonical catalytic triad.^[27]

In-between micellar aggregates and dendrimers lay metallic nanoparticles passivated with a monolayer of functionalized, organic molecules. Because of the clustering of these organic molecules onto the surface of the metallic core, such objects resemble micellar aggregates. However, since their interaction with the metal nanocluster is so strong to be “almost” covalent, they also resemble dendrimers. The obvious advantage with respect to the latter is that organic molecules spontaneously self-assemble on the metallic surface. For instance, gold nanoparticles (AuNPs) are constituted by clusters of gold(0) atoms (ca. 2–50 nm in diameter) passivated with thiolated organic molecules via a strong Au–SR bond. Our contribution to the creation of esterolytic nanozymes was based on the functionalization of small AuNPs with short peptide sequences (Figure 3). Our very first evidence of cooperativity with these nanosystems in the hydrolytic cleavage of a carboxylate ester was obtained with imidazole-functionalized AuNPs.^[28] Analogously to the dendrimers discussed above, the rate vs. pH graph showed a bell-shaped profile indicating that two imidazoles were involved in the catalytic process with complementary roles. AuNPs functionalized with thiols terminating with a HisPhe-OH dipeptide revealed an interesting novelty: a change of mechanism at the low pH regime.^[29] The peptide, incorporated in the nanosystem, showed an increase in activity of at least one order

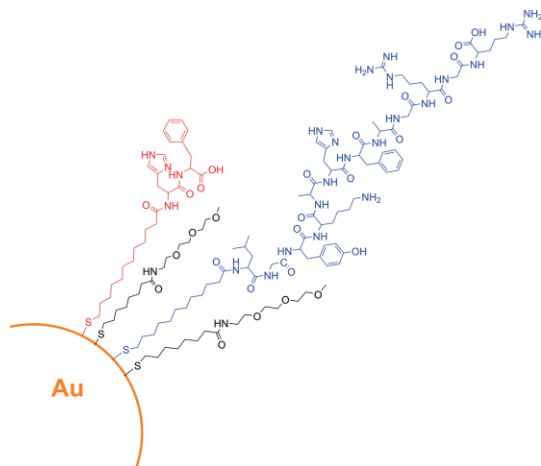


Figure 3. Cartoon representation of a gold nanoparticle (AuNP) with different passivating thiols. In black is a catalytically inactive thiol used for solubilization in an aqueous environment. In red and blue are two different thiols functionalized with different peptides. Each of these AuNPs was used as a nanoesterase (adapted from ref.^[30]).

of magnitude. However, for the monomeric peptide the expected increase in activity was observed upon increasing pH, consistent with the deprotonation of imidazole ($pK_a = 6.6$), the catalytically competent nucleophile while for the nanoparticle a new nucleophilic species appeared with pK_a 4.2, typical of a carboxylic acid. From this experimental evidence we inferred that the confinement of the catalytic units in the monolayer covering the nanoparticles triggered a cooperative hydrolytic mechanism operative at $pH < 7$ in which a carboxylate and an imidazolium ion acted as general base and general acid, respectively. At that low pH that catalytic contribution was absent in the monomeric catalyst thus resulting in a 300-fold rate acceleration for the nanozyme. This reaction pathway seems quite general for AuNPs functionalized with peptides bearing a carboxylate. Indeed, when the dodecapeptide Leu-Gly-Tyr-Lys-Ala-His-Phe-Ala-Gly-Arg-Gly-Arg-OH, presenting a terminal carboxylate was grafted on the nanoparticles, the same cooperative process took place.^[30] The sequence present in this peptide could enable nucleophilic, general-acid, and/or general base catalysis, but also stabilization of the negatively charged transition state that arises along the pathway of ester hydrolysis because of the presence of a His, two Arg, one Tyr and a Lys residue. The pH-rate profile accounted for specific cooperative contributions of the functional groups present in these amino acids playing different roles at different pH values. For instance, at high pH, the activity of the peptide-nanoparticle increased significantly with respect to the previous dipeptide-functionalized nanoparticle as the phenoxide of tyrosine was acting as the nucleophile. The most intriguing result emerged in the regime where the imidazole was the nucleophile. We observed that a lipophilic substrate was able to regulate the activity of the system by shifting the rate-determining step from imidazole acylation to the hydrolysis of this intermediate as a function of its concentration. Such a modulation of the reactivity by the substrate itself is present in many enzymes involved in “cascade” reactions. One interesting property of AuNPs that differentiates them further from micellar aggregates is the precise orientation of the passivating thiols present on the monolayer. This allows one to define with reasonable precision regions of the monolayer where recognition or catalytic events occur. This property was recently exploited by Kokschi et al. who prepared a collection of peptide-functionalized AuNPs in which one of the catalytic functional groups (His) was moved along the peptide sequence from the surface of the monolayer to very close to the gold core (Figure 4).^[31] The 25-mer peptides consisted of three repetitions of seven amino acids, identical but for the sequential replacement of an Ala with a His. Each AuNP was hence very similar to the other but for the position of a single amino acid. By comparing the esterolytic activity against esters of Z-protected amino acids of different lipophilicity (Glu, Ala, Phe and Leu) the authors were able to pinpoint specific regions where the best catalytic performance was achieved. For the most hydrophobic substrates Z-L-Phe and Z-L-Leu maximum rate acceleration was observed when the catalytic site was closest to the gold core of the nanoparticle, i.e. the less hydrated region of the monolayer.^[32] The more hydrophilic ones were best cleaved in the intermediate region and in no case maxi-

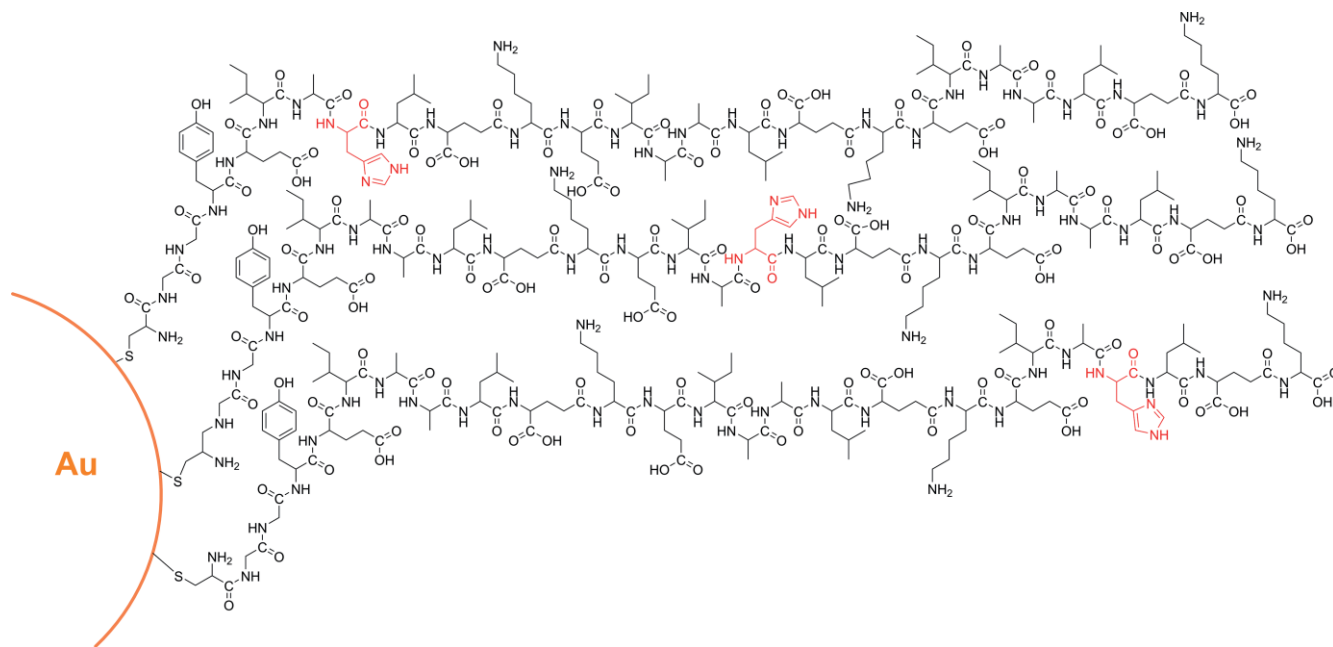


Figure 4. 25-mer peptides used by Kokschi et al. to assess the reaction loci in nanoesterases. Three different AuNPs were prepared each functionalized with a single type of peptide. In each peptide the histidine was placed in different positions: close to the gold(0) core (top), in the centre (middle) and close to the interface with the bulk water (bottom). Adapted from ref.^[31a].

mum activity was observed when the catalytic site was placed in the proximity of the bulk water. These results provide straightforward evidence for the role of desolvation of the nucleophile in the catalytic site as one important source of the rate acceleration observed in hydrolytic nanozymes.^[20]

The same authors studied how the secondary structure of a peptide passivating the AuNP surface could impact on its catalytic efficiency. To this aim they anchored on the surface of gold nanoparticle a peptide catalytically active in the hydrolysis of carboxylate esters. Addition of a complementary helical peptide forming a coiled-coil aggregate and hence inducing a helical conformation to the peptide grafted to the AuNP, almost totally inhibited the activity.^[33] The significant reduction of catalytic efficiency of the conformationally constrained peptide passivating the AuNPs was in part attributed to the intrinsic properties of the added complementary one but also to the more rigid α -helical coiled-coil structure. The authors argued that the flexibility of functional groups leading to productive orientations for substrate binding and catalysis, thus allowing cooperativity between them, were no longer accessible in the structured coiled-coil dimers. We had previously shown that the change of conformation of peptides grafted on a gold cluster surface dramatically changes the interaction of the constituents amino acids with the gold(0) atoms^[34] and may control also AuNPs aggregation.^[35]

Metallic nanoparticles (specifically ceria/polyoxometalates hybrids (CeONP@POMs)) were reported to show proteolytic activity taking advantage of Lewis acid activation of the peptide bond and delivery of nucleophilic hydroxide bound to the metal centers. Interesting results were obtained in the hydrolytic degradation of amyloid- β peptides.^[36] Protein misfolding

to amyloid aggregates is the hallmark for neurodegenerative diseases (like Alzheimer) and, hence, these results might find a role in possible therapeutic applications.

3.2. Templated Nanoesterases

In all the above examples the nanosystem was properly functionalized to assemble the functional groups for the catalytic process to occur. A few years ago, Rotello and Chmielewski^[37] ligated anionic helical peptides on a surface of cationic AuNP, taking advantage of the cooperativity of the interaction related to the multivalency of the interacting species. More recently we took advantage of the same property to self-assemble small negatively charged peptides on their surface.^[38] The peptides contained in their sequence one or more His-residues thus spontaneously self-assembling a catalytic unit where the cationic AuNP was acting as a template. This self-assembled nanocatalyst was able to accelerate the cleavage of Z-protected amino acid esters by more than two orders of magnitude (Figure 5).

At variance with the previous examples where the imidazoles of the His were cooperating in the catalytic process here a linear correlation was observed between the number of His-residues present in the peptides and the second-order rate constant. The pH-rate profile clearly suggested that the role of the imidazoles was that of the nucleophile and not also that of a general acid. Two reasons may account for this: i) the higher local pH originating from the high concentration of the positive charges on the surface^[17] of the nanoparticles leads to the deprotonation of the imidazoles shifting their pK_a to a much lower value;

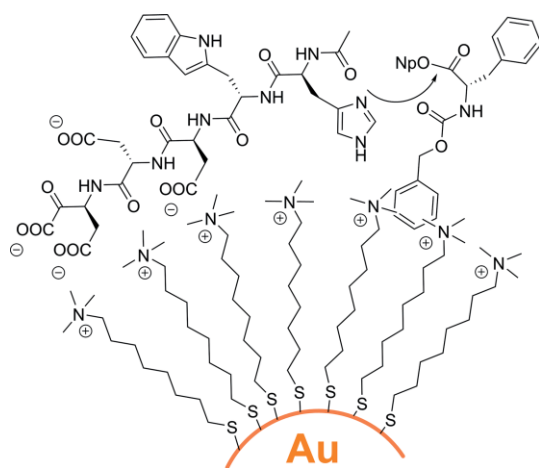


Figure 5. Cationic AuNPs were used as template for the anchoring of an anionic peptide. The ensemble was hence behaving as a catalytic system for the cleavage of the p-nitrophenyl ester of Z-protected phenylalanine (adapted from ref.[38]).

ii) the control of the conformational freedom of the peptide because it sticks to the AuNP surface does not allow two imidazoles to stay close enough to the substrate to take advantage of the cooperativity between them. This is not much different from what was reported by Kokschi in the example discussed above where conformational freedom was reduced by the forced helical conformation of the peptide with consequent loss of cooperativity.

4. Nanocatalysts for the Hydrolysis of Phosphoric Acid Esters

4.1. Nanophosphodiesterases and Nanonucleases

While carboxylate ester hydrolysis constitutes an easy proving ground for nanozyme catalytic efficiency, phosphate esters are quite more challenging, being rather stable compounds. The hydrolysis of a simple phosphate diester as dimethyl phosphate at physiological pH and room temperature proceeds with a half-life of 10^{10} years.^[39] With extraordinary efficiency enzymes accelerate it >16 orders of magnitude.^[39b] Indeed, phosphate-cleaving enzymes are among the most efficient known ones. Most of these enzymes present in their active site catalytically relevant divalent metal ions (like Zn(II), Mg(II)).^[40] The most plausible mechanisms for them require two of these ions operating in a concerted fashion. A critical distance lower than 6.5 Å between metal ions has been estimated to exploit their cooperativity in the catalytic process,^[41–43] although we have recently shown that even metal ions at a longer distance may be catalytically relevant.^[44] All this suggests that the clustering of metal ions on the confined space of a nanosystem may result in powerful synthetic catalysts for the cleavage of phosphate esters. Experimental evidence has demonstrated that this is indeed the case.

Pursuing this idea, back in 2004, we grafted a thiol bearing a triazacyclononane (TACN)-functionalized amino acid^[45] on a gold cluster using a 1:1 mixture with dodecanethiol and tested

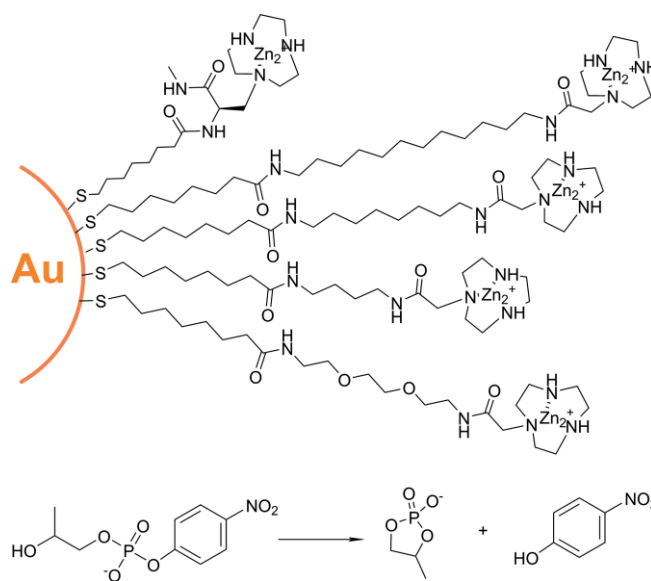


Figure 6. Pictorial representation of the different thiolated ligands used for the preparation of different generations of AuNPs studied for the cleavage of the RNA model substrate HPNPP (adapted from ref.[46] and [52]).

the system for the cleavage of 2-hydroxypropyl p-nitrophenyl phosphate (HPNPP),^[46] a substrate used as a model of RNA. The results were in line with our expectation. The system showed enzyme-like behavior following Michaelis–Menten kinetics and pronounced cooperativity between two Zn(II) ions, a property shared also with other multivalent systems.^[47] For this reason we coined the term “nanozymes” for these nanoparticles (Figure 6).^[48] It should be hardly surprising that also dendrimers functionalized with TACN complexes were excellent catalysts for the cleavage of HPNPP.^[49,50] Third generation DAB (poly(propylene imine)) dendrimers were studied with increasing degree of functionalization (from 0 to 100 % of the peripheral units). The catalytic efficiency increased exponentially with an exponential factor of 2 indicating that the active species was characterized by a dinuclear Zn(II) catalytic site. This appears to be true also for the gold nanoparticles.^[51] Second and third generations of these AuNPs (Figure 6) showed how important the lipophilicity of the monolayer is^[52] and that cationic functional groups, like the guanidinium of Arg, may replace the second metal ion, although with lower efficiency.^[53] For monovalent substrates (i.e. single charged) metal ion-based nanoparticles appear to be better catalysts.^[54] Interestingly, Salvio et al. reported metal-free nanozymes based on guanidium ions for the cleavage of phosphate diesters.^[55,56] The rate vs. pH profiles for these systems were also bell-shaped, indicating cooperation between the guanidine/guanidinium in the catalytic process. In agreement with the results reported above, these systems proved less efficient than those relying on metal ions. The cooperativity of metal ions with other functions has been shown to be an important property of the catalysis of the hydrolysis of phosphate esters.^[57] Being a model of RNA, HPNPP has a built-in nucleophilic hydroxyl that makes its cleavage much faster than that of a normal phosphate ester, like those present in DNA. With these sluggish substrates these complementary functions

present in the catalytic site could prove quite useful. Indeed, by using a ligand in which the action of the metal ion could be assisted by ancillary groups (able to H-bond with the substrate, like bis(2-amino-pyridinyl-6-methyl)amine, BAPA) we prepared Zn(II) nanoparticles very active in the hydrolysis of the DNA model phosphate, bis-p-nitrophenyl phosphate (BNPP).^[58] The advantage of confining the catalytic units on the AuNPs monolayer, thus maximizing the cooperative and hydrophobic contributions, led to a second-order rate constant more than 60,000 higher than that of the base-catalyzed reaction and more than 100-fold better than that of the monomeric complex.

A typical property of natural enzymes is their enantioselectivity. To answer the question whether nanozymes were also able to differentiate enantiomers we have synthesized chiral ligands for the cleavage of chiral RNA model substrates analogous to HPNPP. Thus, thiols containing chiral Zn(II)-binding head groups have been self-assembled on the surface of gold nanoparticles. This resulted in the spontaneous formation of chiral bimetallic catalytic sites that display different activities (determined as k_{cat}) towards the enantiomers of 2-hydroxypropyl p-nitro-m-trifluoromethylphenyl phosphate. Substrate selectivity was observed when the nanozyme was applied to the cleavage of the dinucleotides UpU, GpG, ApA, and CpC, and remarkable differences in reactivity were also observed for the cleavage of the enantiomerically pure dinucleotide UpU.^[59] The selectivities observed were one order of magnitude lower than those typically presented by natural enzymes, nevertheless, they represented one of the few cases reported in the literature of enantioselective phosphate cleavage by a nano catalyst.^[60]

The AuNPs based on the triazacyclononane-Zn(II) complex, in spite of their very good performance in the cleavage of HPNPP, proved quite ineffective in the cleavage of DNA. We attributed this behavior to the multivalency of the natural polymer that upon binding to the metal complexes with its phosphates (a zipper-like interaction) makes it impossible to create a dinuclear catalytic site. However, the nanoparticles functionalized with the BAPA-Zn(II) complex and very effective in the cleavage of BNPP (see above) were active both as a dinuclear and mononuclear complex, although the dinuclear one was more efficient. We argued that these AuNPs could prove excellent candidates for the cleavage of DNA because cooperativity between two metal ions was not a prerequisite for their activity. This turned out to be the case (Figure 7). Not only they were fairly active in plasmid DNA cleavage but they were able to cleave the polymer on both strands, a property hardly shown by synthetic catalysts (Figure 7).^[58] These AuNPs appear to be an interesting case of a processive catalyst,^[61] as very likely the gold nanoparticles roll over the polymer cleaving the phosphate bonds they interact with. Impressive rate accelerations in the cleavage of BNPP, and DNA as well, were also reported by König^[62] who showed that micelles and vesicles from amphiphilic Zn(II)-cyclen complexes were extremely active. In the case of DNA, cleavage was observed not only with the plasmid but also with smaller, typically much less reactive, single-strand fragments. For the pBR322 plasmid DNA, both a conversion of the supercoiled to the relaxed and linear form, and also a further degradation into smaller fragments by double strand cleav-

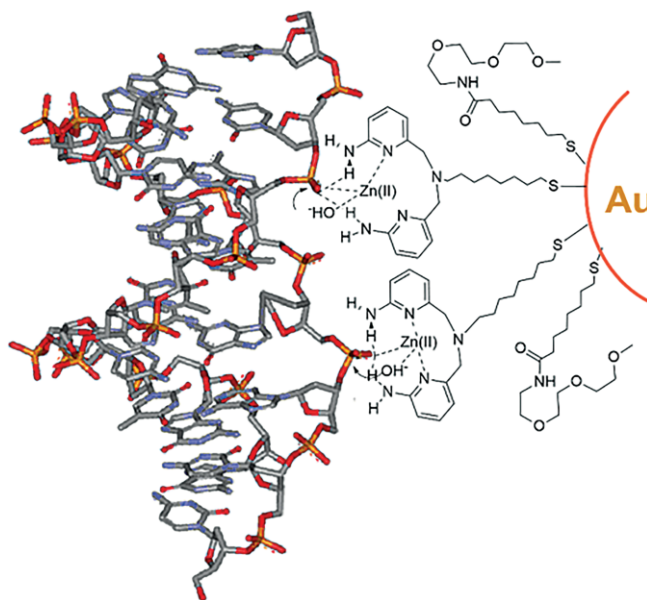


Figure 7. Possible mode of interaction between a AuNP functionalized with bis(2-amino-pyridinyl-6-methyl)amine, BAPA, Zn(II) complexes and dsDNA. This nanozyme cleaves dsDNA on both strands possibly via a processive catalytic mechanism (adapted from ref.^[58]).

ages could be observed after incubation with the vesicular Zn(II) complexes.

The cleavage of phosphate triesters deserves a specific consideration. These compounds are more reactive than phosphate diesters because they are neutral species and, hence, react more readily with an incoming negatively charged nucleophile.

The interest in these compounds is connected to the fact that they are simulants of noxious chemical weapons: nerve agents. Developing catalysts capable to cleave them could contribute to the safe destruction of stockpiles of these weapons and to the decontamination of contaminated areas. Nanozymes were designed for tackling this problem using micellar and vesicular aggregates many years ago.^[63,64] The results were quite interesting and resulted in the implementation of some of these systems for actual applications. The strong Lewis acid properties of ceria nanoparticles were also exploited for the hydrolysis of these substrates.^[65] More recently a new generation of effective catalysts were introduced based on metal organic frameworks (MOFs).^[66–68] MOFs constitute a broad class of crystalline materials comprising an array of metal-containing nodes separated by organic linkers. Their catalytic properties derive from the ability to both bind and transform substrates. They are, hence, nanozymes working under heterogeneous conditions. Because of their ability to present high concentrations of metal ions dispersed in structurally well-defined structures they may exploit the cooperativity between functional groups. The Zr₆-based MOF, NU-1000, has a structure in which a total of four terminal-zirconium-ligated aquo and hydroxo groups per node form 31 Å channels that allow molecules, like phosphate esters, to permeate their interior for hydrolytic degradation (Figure 8). NU-1000 hydrolyzes the nerve agent simulant dimethyl p-nitrophenyl phosphate (DMNP) with $t_{1/2} = 1.5$ min (vs. a mere 3 % conversion after 60 min in the absence of catalyst). The Lewis

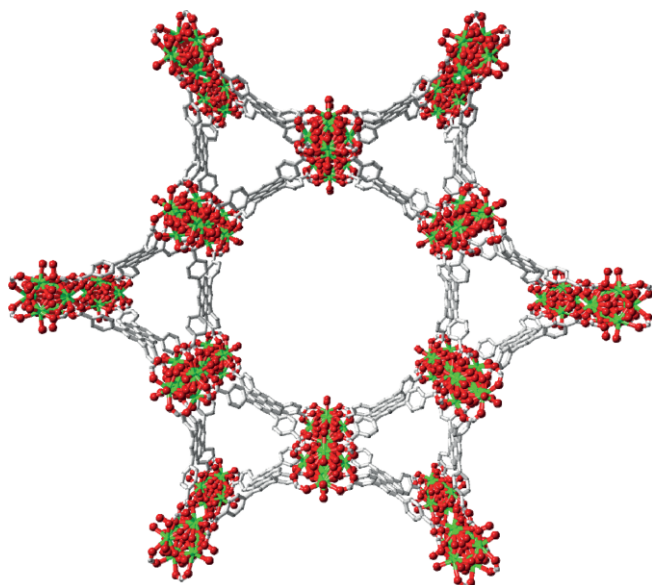


Figure 8. The Zr₆-based MOF, NU-1000. In colours the catalytically pertinent metal cluster. The picture shows clearly the cavity available for the substrate to be transformed (courtesy Prof. Omar K. Farha, Northwestern University, USA).

acid properties of the Zr groups are of key importance for the catalytic transformation.

4.2. Exploiting Nanonucleases for Sensing and Reactivity Control

We have shown that cationic nanoparticles present a very high affinity for oligoanions, like polyanionic peptides and DNA. The same applies to ATP, ADP and other oligophosphates. In line with what is known for the affinity constants between oligo cations and anions, the affinity of the oligoanions for the catalytic monolayer surface of a gold nanoparticle is strictly related to the number of negative charges of the probe.^[69] Obviously, the higher the net charge of a probe, the larger its affinity constant for the AuNP surface. If the cationic surface of the nanoparticle is constituted by TACN-Zn(II) complexes, catalytically active in the cleavage of HPNPP, these polyanions may act as inhibitors of the catalytic process by displacing the less charged substrate from the surface itself. This property was exploited for detecting the activity of an enzyme able to cleave these anions (a protease for anionic polypeptides or an ATPase for ATP and ADP), see Figure 9.^[70] The assay relies on the fact that the enzyme substrate and HPNPP compete for the surface of the nanoparticle with the enzyme substrate showing far higher affinity thus inhibiting the cleavage of HPNPP. Upon hydrolysis by the enzyme of the inhibitor (which is a substrate for the enzyme) the catalytic activity of the AuNPs against HPNPP is restored,^[70,71] resulting in the production of the p-nitrophenolate anion as a reporter of the activity of the enzyme. Since the detection of the enzyme relies on two catalytic processes, there is quite significant signal amplification associated with high sensitivity as the intensity of the output is connected to the turn-over number of both catalysts, the AuNPs and the enzyme

(double amplification). Noteworthy, since the inhibition is present only as long as the polyanionic substrate is present, they can be considered as “regulators” of the activity of the nanozyme.^[71] The same AuNPs were used to discriminate ATP from ADP also by means of catalytic signal amplification.^[72] In this case the substrate used as a chromogenic reporter, following its cleavage by AuNPs, was 2-hydroxypropyl-(3-trifluoromethyl-4-nitro)phenyl phosphate, more reactive than HPNPP. It was this increased affinity for the nanoparticle surface that allowed for the discrimination between ATP and ADP. In fact, this phosphate was able to compete with ATP and ADP to different extents for binding on the monolayer surface, thus enabling a catalytically amplified signal only when ATP was absent. The discrimination between ATP and ADP is of relevance for the development of universal assays for the detection of enzymes which consume ATP. For example, protein kinases are a class of enzymes critical for the regulation of cellular functions, and act to modulate the activity of other proteins by transphosphorylation, transferring a phosphate group from ATP to give ADP as a by-product.

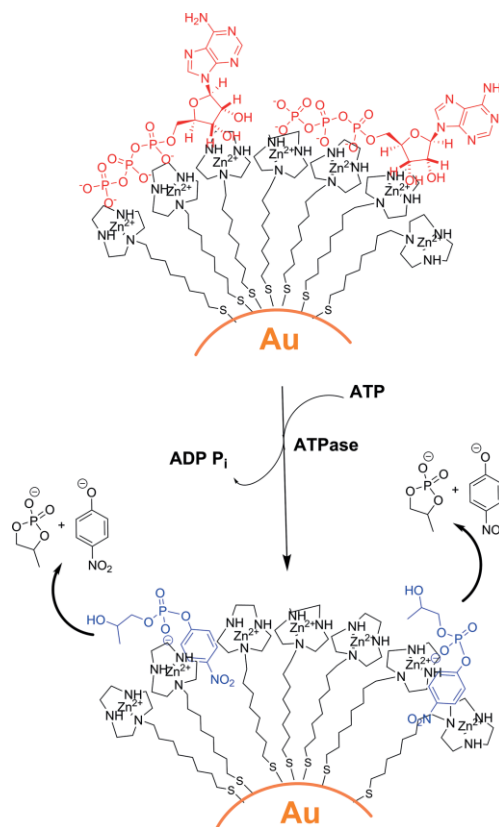


Figure 9. Sensing of an ATPase by nanozymes following a double amplification protocol. Top: ATP inhibited nanozyme; bottom: active nanozyme after hydrolysis of the ATP inhibitor. The release of p-nitrophenol allows the indirect colorimetric detection of the ATPase responsible of the activation of the nanozyme (adapted from ref.^[70]).

The interaction of the catalytic units present on the surface of TACN-Zn(II)-functionalized nanoparticles with “tunable” inhibitors was exploited by Neri et al. to switch on and off their activity.^[73] The switchable inhibitor was 4-(phenylazo)-benzoic acid, because it combines a photoresponsive azobenzene and

a carboxylic acid group, which is negatively charged at pH 7.0 and, hence, able to interact with the metal complex. The azo dye can be reversibly switched between two photostationary states (trans/cis = 35:65 after irradiation at $\lambda = 365$ nm for 50 min, trans/cis = 77:23 after irradiation at $\lambda = 465$ nm for 10 min) with the trans isomer having an higher affinity for the metal complexes present on the AuNPs monolayer. This difference in affinity resulted in the displacement of HPNPP with inhibition of its cleavage by the trans isomer but not by the cis one. Accordingly, catalytic activity of the AuNPs could be reversibly controlled by light irradiation at the proper wavelength.

We used the interaction with polyanions like ATP to transiently stabilize vesicular systems. In the presence of an ATPase the vesicles can only exist if the system is continuously “fed” with ATP itself. Accordingly, the system dissipates energy to exist and consumes the “chemical fuel” ATP.^[74] This was an outstanding example of dissipative self-assembled nanosystem relying on an hydrolytic process occurring at the vesicular/bulk water interface where the TACN-Zn(II) complexes, binding ATP, reside. Quite interesting for the scope of this review is an example reported by Chen et al.,^[75] relying on the same principle, where the substrate HPNPP was the trigger of the formation of the aggregates constituted by lipophilic TACN-Zn(II) complexes. The formation of aggregates installs the dinuclear catalytic site that efficiently cleaves HPNPP itself (Figure 10). Thus, this very same substrate induced the “suicidal” formation of the catalysts that was going to kill it. The difference in the ability to induce aggregation by HPNPP and its cleavage product, the cyclic phosphate 4-methyl-1,3,2-dioxaphospholan-2-olate-2-oxide, although small, allowed the aggregation/disaggregation of the catalytic assemblies following the addition/hydrolysis of HPNPP. The substrate HPNPP represents the “chemical fuel” that keeps the nanozyme alive. The same nanozyme consumes this fuel leading to its partial disruption via disaggregation.

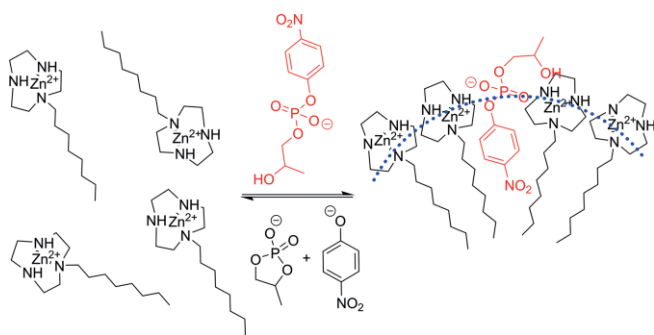


Figure 10. Substrate-induced formation of aggregates. The cleavage of the substrate reverts back the system to unaggregated monomers. The nanozyme exists only as long as the system is fed with the substrate. The dotted blue line represents the interfacial region between aggregate and bulk water (adapted from ref.^[75]).

By using different AuNPs functionalized with TACN-Zn(II) or 1,4,7,10-tetraaza-cyclododecane (cyclen)-Zn(II) complexes Della Sala et al. were able to selectively recognize different nucleobases in a selective manner.^[76] Thus the AuNPs based on the TACN-Zn(II) complexes were selective for guanine monophosphate (GMP) while those based on cyclen-Zn(II) complexes were

selective for thymidine monophosphate (TMP) allowing their specific complexation on the surface out of a mixture of four different nucleotides (GMP, TMP, adenosine monophosphate, AMP, and cytidine monophosphate, CMP). The binding process was controlled by alkaline phosphatase that by cleaving the AuNP-bound nucleobase was making the surface available for a subsequent binding event. In case this binding event involved a fluorescent dye, its fluorescence could be turned on (unbound) or off (bound) following the hydrolytic process occurring on the AuNPs surface and catalyzed by the enzyme.

Summary and Outlook

Nanosystems are excellent hydrolytic catalysts with properties similar to those of natural enzymes. For this reason, they have been dubbed “nanozymes”.^[46] All of them share the ability to bind the substrate before its transformation. The confinement of several functional groups in a limited space provides the conditions for inducing cooperativity between them, a property difficult to install in classical molecular catalysts. In many cases they also provide an environment different from that of the bulk solvent (typically water) where they are dispersed by changing the local pH, the solvation of the substrate and, more important, that of the transition state. Their catalytic performance is strongly related to their properties. Thus, micellar (and vesicular) aggregates are very simple to prepare but their existence strongly depends on the properties of the solvent, the ionic strength of the solution and the presence of additives. The control of the topology and of the properties of the reaction loci is very limited in these systems. Their catalytic performance is, accordingly, limited. On the opposite site lay dendrimers. They are synthetically challenging nanosystems but, once prepared, they allow a fairly precise control of the properties of the catalytic site. Metal-nanoparticles (like AuNPs) represent a good compromise between the previous two nanosystems. They are relatively easy to prepare and allow a reasonably good control of the properties of the catalytic site. Rate accelerations with these systems may be impressive. It should thus not be surprising to see how popular they have become. An interesting new class of nanocatalysts is constituted by metal organic frameworks. They are simple to prepare but a possible limitation for them could be the limited variability in the introduction of different functions in the catalytic site.

Table 2 reports the kinetic parameters (as discussed in Section 2) for most of the above nanozymes in the cleavage of HPNPP (see Figure 6) featuring the very same TACN-Zn(II) function in the catalytic site. It allows one to make a comparison between them. The k_{rel} , the ratio between second order rate constants (or k_{cat}/K_M) shows how the best nanozyme is constituted by AuNPs followed by dendrimers while the micellar aggregates are the worst. One may ask why dendrimers perform worse than AuNPs. One possible reason is that those reported (the only ones for which reliable data are available) are much more hydrated than AuNPs. It is well known that a lower-polarity catalytic site favors a better catalytic performance.^[52] Considering the effort that has been put in the preparation of a dendrimer, AuNPs appear a better (certainly easier to obtain)

Table 2. Kinetic parameters for the cleavage of HPNPP by different TACN-Zn(II)-functionalized nanozymes and reference reactions.

Catalyst	K_M , mM	k_{cat} , s ⁻¹	k_{cat}/k_{uncat} ^[a]	k_{cat}/K_M , M ⁻¹ × s ⁻¹	k_{rel} ^[b]	Ref
OH ⁻	–	–	–	9.8×10^{-4} ^[c]	1	[77]
TACN-Zn(II)	–	–	–	0.022 ^[d]	22	[78]
Micelle ^[e,f]	0.53	0.003	15000	5.7	5814	[75]
AuNP ^[g,h]	0.58	0.030	150000	51.7	52755	[53]
Dendrimer ^[h,i]	0.8	0.016	80000	19.0	19396	[50]

[a] k_{uncat} : 2.0×10^{-7} s⁻¹, pH = 8, 40 °C. [b] Relative second order rate. [c] At 25 °C. [d] Second order rate constant. [e] 1-nC₁₈H₃₅-TACN-Zn(II) surfactant. [f] At pH 7.0 and 40 °C. [g] 1-(8-mercaptopentyl)-TACN-Zn(II) ligand on AuNP. [h] At pH 7.5 and 40 °C. [i] Branched polylysine dendrimer with 32 TACN-Zn(II) units.

choice. The poorer catalytic performance of micellar aggregates was fully predictable on the bases of what stated above. As Menger pointed out:^[9] “enzyme-like rates can occur when two reactants are held rigidly at favorable geometries and at close “contact distances” (defined as less than 3 Å, the diameter of water)”. This is a situation almost impossible to achieve with micellar aggregates considering the very fast exchange rate between monomers and aggregate.

An often overlooked aspect of the catalysis with nanozymes is how the substrate itself may modulate the properties of the catalytic site up to the point of inducing its formation.^[75] More often it may change its polarity^[30] or the relative disposition of the functional groups.^[19,30] Preliminary results from our group show, for instance, that the assessment of a catalyst against a monovalent substrate cannot be extended to a polyvalent one. A case in point is constituted by a monovalent phosphate diester often used as a model for DNA cleavage. Excellent catalysts for the monovalent substrate may, disappointingly, turn out to be not as good for the multivalent ones. This is because the interaction between a multivalent catalyst with a multivalent substrate is quite different from that with a monovalent one.

We believe the field is still developing and new nanosystems with improved catalytic efficiencies and selectivities will appear in the near future. As the data of Table 2 indicate, monolayer-passivated nanoparticles constitute one of the best choices as they permit the introduction in their catalytic sites of several functions allowing a more sophisticated mimicry of the catalytic site of an enzyme.

Acknowledgments

The authors thank the many students and post-docs who, with their passion, intelligence and dedication contributed to the work reported here. Their names are reported in the references quoting the work from our own group. PS thanks MIUR (Rome, project PRIN, grant 2015RNWJAM) and the EU (Marie Curie program MSCA-ITN-2016, project MMBio, grant 721613) for financial support.

Keywords: Nanozymes · Enzyme mimic · Nanoesterase · Nanonuclease · Hydrolysis

[1] Y. Huang, J. Ren, X. Qu, *Chem. Rev.* **2019**, *119*, 4357–4412.

[2] D. Jiang, D. Ni, Z. Rosenkrans, P. Huang, X. Yan, W. Cai, *Chem. Soc. Rev.* **2019**, *48*, 3683–3704.

[3] M. Liang, X. Yan, *Acc. Chem. Res.* **2019**, *52*, 2190–2200.

[4] W. Chen, S. Li, J. Wang, K. Sun, Y. Si, *Nanoscale* **2019**, *11*, 15783–15793.

[5] T. Kang, Y. Kim, D. Kim, T. Hyeon, *Coord. Chem. Rev.* **2020**, *403*, 213092.

[6] C. Fasting, C. Schalley, M. Weber, O. Seitz, S. Hecht, B. Koksche, J. Drenedde, C. Graf, E. Knapp, R. Haag, *Angew. Chem. Int. Ed.* **2012**, *51*, 10472–10498.

[7] A. Barnard, D. Smith, *Angew. Chem. Int. Ed.* **2012**, *51*, 6572–81.

[8] R. Haag, *Beilstein J. Org. Chem.* **2015**, *11*, 848–849.

[9] F. Menger, F. Nome, *Acc. Chem. Biol.* **2019**, *14*, 1386–1392.

[10] C. A. Hunter, H. L. Anderson, *Angew. Chem. Int. Ed.* **2009**, *48*, 7488–7499.

[11] C. Matassini, C. Parmeggiani, F. Cardona, A. Goti, *Tetrahedron Lett.* **2016**, *57*, 5407–5415.

[12] Nothling, A. Ganesan, K. Condit-Jurkic, E. Pressly, A. Davalos, M. Gotrik, Z. Xiao, E. Khoshdel, C. Hawker, M. O'Mara, et al., *Chem* **2017**, *2*, 732–745.

[13] F. Hollfelder, A. Kirby, D. Tawfik, *J. Org. Chem.* **2001**, *66*, 5866–5874.

[14] a) E. J. Fendler, J. H. Fendler, *Catalysis in Micellar and Macromolecular Systems*, Academic Press, London, **1975**; b) J. H. Fendler, *Membrane Mimetic Chemistry: Characterizations and Applications of Micelles, Microemulsions, Monolayers, Bilayers, Vesicles, Host-Guest Systems, and Polyions*, Wiley, New York, **1982**.

[15] M. Nothling, Z. Xiao, A. Bhaskaran, M. Blyth, C. Bennett, M. Coote, L. Connal, *Acc. Chem. Res.* **2019**, *9*, 168–187.

[16] a) S. Serrano-Luginbühl, K. Ruiz-Mirazo, R. Ostaszewski, F. Gallou, P. Walde, *Nat. Rev. Chem.* **2018**, *2*, 306–327; b) M. Khan, I. Fagge, *Prog. React. Kinet. Mec.* **2018**, *43*, 1–20; c) G. Sorella, G. Strukul, A. Scarso, *Green Chem.* **2015**, *17*, 644–683; d) F. Mancin, P. Scrimin, P. Tecilla, U. Tonellato, *Coord. Chem. Rev.* **2009**, *253*, 2150–2165.

[17] C. Bunton, F. Nome, F. Quina, L. Romsted, *Acc. Chem. Res.* **1991**, *24*, 357–364.

[18] L. Romsted, C. Bunton, J. Yao, *Curr. Opin. Colloid* **1997**, *2*, 622–628.

[19] a) P. Scrimin, P. Tecilla, U. Tonellato, *J. Org. Chem.* **1994**, *59*, 4194–4201; b) G. Santi, P. Scrimin, U. Tonellato, *Tetrahedron Lett.* **1990**, *31*, 4791–4794.

[20] A. Warshel, *Angew. Chem. Int. Ed.* **2014**, *53*, 10020–10031.

[21] Y. Ding, N. Williams, C. Hunter, *J. Am. Chem. Soc.* **2019**, *141*, 17847–17853.

[22] J. M. J. Frechet, *Proc. Natl. Acad. Sci. USA* **2002**, *99*, 4782–4787.

[23] X. Fan, Z. Li, X. Loh, *Polym. Chem.* **2016**, *7*, 5898–591.

[24] a) E. Delort, T. Darbre, J.-L. Reymond, *J. Am. Chem. Soc.* **2004**, *126*, 15642–15643; b) T. Darbre, J. L. Reymond, *Acc. Chem. Res.* **2006**, *39*, 925–934; c) J. Kofoed, J. L. Reymond, *Curr. Opin. Chem. Biol.* **2005**, *9*, 656–664.

[25] J.-L. Reymond, T. Darbre, *Chimia* **2013**, *67*, 864–867.

[26] See ref.^[24a].

[27] See ref.^[12].

[28] L. Pasquato, F. Rancan, P. Scrimin, F. Mancin, C. Frigeri, *Chem. Commun.* **2000**, 2253–2254.

[29] P. Pengo, S. Polizzi, L. Pasquato, P. Scrimin, *J. Am. Chem. Soc.* **2005**, *127*, 1616–1617.

[30] P. Pengo, L. Baltzer, L. Pasquato, P. Scrimin, *Angew. Chem. Int. Ed.* **2007**, *46*, 400–404.

[31] a) D. J. Mikolajczak, J. Scholz, B. Koksche, *ChemCatChem* **2018**, *10*, 5665–5668; b) D. Mikolajczak, A. Berger, B. Koksche, *Angew. Chem. Int. Ed.* **2020**, DOI-10.1002/anie.201908625.

[32] L. Riccardi, L. Gabrielli, X. Sun, F. De Biasi, F. Rastrelli, F. Mancin, M. De Vivo, *Chem* **2017**, *3*, 92–109.

[33] D. J. Mikolajczak, J. L. Heier, B. Schade, B. Koksche, *Biomacromolecules* **2017**, *18*, 3557–3562.

- [34] E. Longo, A. Orlandin, F. Mancin, P. Scrimin, A. Moretto, *ACS Nano* **2013**, 7, 9933–9939.
- [35] Y. Lyu, G. Marafon, Á. Martínez, A. Moretto, P. Scrimin, *Chem. Eur. J.* **2019**, 25, 11758–11764.
- [36] a) Y. Guan, M. Li, K. Dong, N. Gao, J. Ren, Y. Zheng, X. Qu, *Biomaterials* **2016**, 98, 92–102; b) N. Gao, K. Dong, A. Zhao, H. Sun, Y. Wang, J. Ren, X. Qu, *Nano Res.* **2016**, 9, 1079–1090.
- [37] Y. Fillon, A. Verma, P. Ghosh, D. Ernenwein, V. M. Rotello, J. Chmielewski, *J. Am. Chem. Soc.* **2007**, 129, 6676–6677.
- [38] a) D. Zaramella, P. Scrimin, L. J. Prins, *J. Am. Chem. Soc.* **2012**, 134, 8396–8399; b) D. Zaramella, P. Scrimin, L. J. Prins, *Int. J. Mol. Sci.* **2013**, 14, 2011–2021.
- [39] a) R. Wolfenden, *Chem. Rev.* **2006**, 106, 3379–3396; b) R. Wolfenden, *Ann. Rev. Biochem.* **2011**, 80, 645–667.
- [40] a) M. Diez-Castellnou, A. Martinez, F. Mancin, *Adv. Phys. Org. Chem.* **2017**, 51, 129–186; b) G. Palermo, A. Cavalli, M. Klein, M. Alfonso-Prieto, M. Peraro, M. De Vivo, *Acc. Chem. Res.* **2015**, 48, 220–228; c) F. Mancin, P. Scrimin, P. Tecilla, *Chem. Commun.* **2012**, 48, 5545–5559; d) C. M. Dupureur, *Curr. Chem. Biol.* **2008**, 12, 250–255; e) N. Mitić, S. J. Smith, A. Neves, L. W. Guddat, L. R. Gahan, G. Schenk, *Chem. Rev.* **2006**, 106, 3338–3363; f) M. J. Jedrzejewski, P. Setlow, *Chem. Rev.* **2001**, 101, 607–618; g) J. A. Cowan, *Chem. Rev.* **1998**, 98, 1067–1087; h) D. E. Wilcox, *Chem. Rev.* **1996**, 96, 2435–2458.
- [41] P. Rossi, F. Felluga, P. Tecilla, F. Formaggio, M. Crisma, C. Toniolo, P. Scrimin, *J. Am. Chem. Soc.* **1999**, 121, 6948–6949.
- [42] B. Bauer-Siebenlist, F. Meyer, E. Farkas, D. Vidovic, S. Dechert, *Chem. Eur. J.* **2005**, 11, 4349–4360.
- [43] D. Bim, E. Svobodová, V. Eigner, L. Rulišek, J. Hodačová, *Chem. Eur. J.* **2016**, 22, 10426–10437.
- [44] E. Bencze, C. Zonta, F. Mancin, L. Prins, P. Scrimin, *Eur. J. Org. Chem.* **2018**, 2018, 5375–5381.
- [45] P. Rossi, F. Felluga, P. Scrimin, *Tetrahedron Lett.* **1998**, 39, 7159–7162.
- [46] F. Manea, F. Bodar-Houillon, L. Pasquato, P. Scrimin, *Angew. Chem. Int. Ed.* **2004**, 43, 6165–6169.
- [47] A. Scarso, G. Zaupa, F. B. Houillon, L. J. Prins, P. Scrimin, *J. Org. Chem.* **2007**, 72, 376–85.
- [48] L. Pasquato, P. Pengo, P. Scrimin, *Supramol. Chem.* **2005**, 17, 163–171.
- [49] M. Martin, F. Manea, R. Fiammengio, L. J. Prins, L. Pasquato, P. Scrimin, *J. Am. Chem. Soc.* **2007**, 129, 6982–6983.
- [50] G. Zaupa, P. Scrimin, L. J. Prins, *J. Am. Chem. Soc.* **2008**, 130, 5699–5709.
- [51] G. Zaupa, C. Mora, R. Bonomi, L. J. Prins, P. Scrimin, *Chem. Eur. J.* **2011**, 17, 4879–4889.
- [52] M. Diez-Castellnou, F. Mancin, P. Scrimin, *J. Am. Chem. Soc.* **2014**, 136, 1158–61.
- [53] J. Czeszcik, S. Zamolo, T. Darbre, F. Mancin, P. Scrimin, *Molecules* **2019**, 24, 2814.
- [54] a) M. Manto, P. Xie, C. Wang, *Acs Catal.* **2017**, 7, 1931–1938; b) R. Bonomi, P. Scrimin, F. Mancin, *Org. Biomol. Chem.* **2010**, 8, 2622–2626.
- [55] R. Salvio, A. Cincotti, *Rsc Adv.* **2014**, 4, 28678–28682.
- [56] C. Savelli, R. Salvio, *Chem. Eur. J.* **2015**, 21, 5856–5863.
- [57] a) G. Q. Feng, J. C. Mareque-Rivas, R. T. M. de Rosales, N. H. Williams, *J. Am. Chem. Soc.* **2005**, 127, 13470–13471; b) G. Q. Feng, J. C. Mareque-Rivas, N. H. Williams, *Chem. Commun.* **2006**, 1845–1847; c) G. Q. Feng, D. Natale, R. Prabakaran, J. C. Mareque-Rivas, N. H. Williams, *Angew. Chem. Int. Ed.* **2006**, 45, 7056–7059; d) M. Livieri, F. Mancin, G. Saielli, J. Chin, U. Tonellato, *Chem. Eur. J.* **2007**, 13, 2246–2256; e) M. Livieri, F. Mancin, U. Tonellato, J. Chin, *Chem. Commun.* **2004**, 2862–2863.
- [58] R. Bonomi, F. Selvestrel, V. Lombardo, C. Sissi, S. Polizzi, F. Mancin, U. Tonellato, P. Scrimin, *J. Am. Chem. Soc.* **2008**, 130, 15744–15745.
- [59] J. Chen, C. Pezzato, P. Scrimin, L. Prins, *Chem. Eur. J.* **2016**, 22, 7028–7032.
- [60] R. Zhang, Y. Zhou, X. Yan, K. Fan, *Microchim. Acta* **2019**, 186, 782.
- [61] S. van Dongen, J. Elemans, A. Rowan, R. Nolte, *Angew. Chem. Int. Ed.* **2014**, 53, 11420–11428.
- [62] B. Gruber, E. Kataev, J. Aschenbrenner, S. Stadlbauer, B. König, *J. Am. Chem. Soc.* **2011**, 133, 20704–20707.
- [63] H. Morales-Rojas, R. A. Moss, *Chem. Rev.* **2002**, 102, 2497–2522.
- [64] F. M. Menger, L. H. Gan, E. Johnson, D. H. Durst, *J. Am. Chem. Soc.* **1987**, 109, 2800–2803.
- [65] A. Vernekar, T. Das, G. Muges, *Angew. Chem. Int. Ed.* **2015**, 55, 1412–1416.
- [66] A. Howarth, M. Majewski, O. K. Farha, *Metal-Organic Frameworks for Capture and Detoxification of Nerve Agents*, in *Metal-Organic Frameworks (MOFs) for Environmental Applications* (Ed.: S. K. Ghosh), Elsevier, **2019**.
- [67] J. Mondloch, M. Katz, W. III, P. Ghosh, P. Liao, W. Bury, G. Wagner, M. Hall, J. DeCoste, G. Peterson, R. Q. Snurr, C. J. Cramer, J. T. Hupp, O. K. Farha, *Nat. Mater.* **2015**, 14, 512–516.
- [68] M. Katz, J. Mondloch, R. Totten, J. Park, S. Nguyen, O. Farha, J. Hupp, *Angew. Chem. Int. Ed.* **2014**, 53, 497–501.
- [69] L. Prins, *Acc. Chem. Res.* **2015**, 48, 1920–1928.
- [70] R. Bonomi, A. Cazzolaro, A. Sansone, P. Scrimin, L. J. Prins, *Angew. Chem. Int. Ed.* **2011**, 50, 2307–2312.
- [71] C. Pezzato, L. Prins, *Nat. Commun.* **2015**, 6, 7790.
- [72] C. Pezzato, J. Chen, P. Galzerano, M. Salvi, L. Prins, *Org. Biomol. Chem.* **2016**, 14, 6811–6820.
- [73] S. Neri, S. Martin, C. Pezzato, L. Prins, *J. Am. Chem. Soc.* **2017**, 139, 1794–1797.
- [74] S. Maiti, I. Fortunati, C. Ferrante, P. Scrimin, L. Prins, *Nat. Chem.* **2016**, 8, 725–731.
- [75] P. Muñana, G. Ragazzon, J. Dupont, C. Ren, L. Prins, J. Chen, *Angew. Chem. Int. Ed.* **2018**, 57, 16469–16474.
- [76] F. della Sala, S. Maiti, A. Bonanni, P. Scrimin, L. Prins, *Angew. Chem. Int. Ed.* **2018**, 57, 1611–1615.
- [77] N. Williams, B. Takasaki, M. Wall, J. Chin, *Acc. Chem. Res.* **1999**, 32, 485–493.
- [78] M. Diez-Castellnou, G. Salassa, F. Mancin, P. Scrimin, *Front Chem.* **2019**, 7, 469.

Received: March 17, 2020